

ARTICLE

First-Principles Study of Pd Single-Atom Catalysis to Hydrogen Desorption Reactions on MgH₂(110) Surface

Xin-xing Wu, Wei Hu*

Hefei National Laboratory for Physical Sciences at the Microscale, University of Science and Technology of China, Hefei 230026, China

(Dated: Received on September 29, 2018; Accepted on November 20, 2018)

MgH₂ is a promising and popular hydrogen storage material. In this work, the hydrogen desorption reactions of a single Pd atom adsorbed MgH₂(110) surface are investigated by using first-principles density functional theory calculations. We find that a single Pd atom adsorbed on the MgH₂(110) surface can significantly lower the energy barrier of the hydrogen desorption reactions from 1.802 eV for pure MgH₂(110) surface to 1.154 eV for Pd adsorbed MgH₂(110) surface, indicating a strong Pd single-atom catalytic effect on the hydrogen desorption reactions. Furthermore, the Pd single-atom catalysis significantly reduces the hydrogen desorption temperature from 573 K to 367 K, which makes the hydrogen desorption reactions occur more easily and quickly on the MgH₂(110) surface. We also discuss the microscopic process of the hydrogen desorption reactions through the reverse process of hydrogen spillover mechanism on the MgH₂(110) surface. This study shows that Pd/MgH₂ thin films can be used as good hydrogen storage materials in future experiments.

Key words: Hydrogen storage, MgH₂(110) surface, Pd single-atom catalysis, Hydrogen desorption reaction

I. INTRODUCTION

With high energy density and combustion without pollution, hydrogen gas (H₂) is considered to be a highly efficient, environmentally friendly and clean energy source. The safe, efficient, convenient, and economic storage of hydrogen energy is an important research area, and has received a lot of research attentions in recent 30 years, including solid, liquid, and gaseous hydrogen storage materials [1]. Magnesium hydride (MgH₂) has a high hydrogen capacity of 7.6 wt%, and is solid at room temperature and atmospheric pressure (298 K and 1 bar). Therefore, MgH₂ is a promising and popular hydrogen storage material used in the experiments.

However, the hydrogen adsorption and desorption reactions of MgH₂ are too slow. And a high temperature of 573 K (300 °C) is required to release hydrogen gas. To conquer this shortcoming, several experimental techniques have been used to enhance the hydrogen storage performance of MgH₂, such as doping, alloys, catalysts, composites, and nanomaterials (nanoparticles, nanowires, thin films) [2–5]. In particular, the synthesis of Mg/MgH₂ thin films is an effective method to improve the hydrogen storage performance [6–25]. At

the earlier time, Fujii *et al.* have synthesized the Pd/Mg thin films successfully, and investigated the hydrogen adsorption and desorption properties [6]. Singh *et al.* have reported that during the hydrogenation and dehydrogenation process of Pd/Mg thin films, the structural change relationship is the Mg(0001) surface respect to the MgH₂(110) surface [7]. This relationship has also been confirmed by other experimental studies [24]. Qu *et al.* have systematically investigated the hydriding and dehydriding properties of Pd/Mg thin films, and revealed that the thin films could absorb and desorb H₂ quickly [8, 10, 11, 16]. Xin *et al.* have experimentally synthesized a series of Pd/Mg, Pd/Al/Mg and Pd/Ti/Mg thin films, and the minimum hydrogen desorption energy barrier of about 44 kJ/mol was observed for the best performed Pd/Ti/Mg thin films [13, 14, 17, 18]. Furthermore, Pd nanoparticles covered Mg thin films show good hydrogen adsorption properties, and the hydrogen adsorption mechanism was considered to be the hydrogen spillover mechanism [20, 24]. Therefore, Pd is an excellent catalyst for Pd/Mg based hydrogen storage materials. Furthermore, it has been reported that Pd/Mg thin films based devices could have some applications in the area of hydrogen sensors and detectors [26]. Recently, Pd/Ti/Mg thin films based devices have been designed in potential applications, such as plasmonic materials, plasmonic color printing, and dynamic plasmonic color displays [27, 28].

On the other hand, many theoretical researches on the hydrogen desorption properties of pure and metals

* Author to whom correspondence should be addressed. E-mail: whuustc@ustc.edu.cn

doped MgH₂(110) surface have been reported [29–35]. These theoretical studies mainly focus on the calculations of the hydrogen desorption energies in the aspect of thermodynamic, and only several theoretical studies refer to the calculations of the hydrogen desorption energy barriers in the aspect of kinetic [29, 31, 33, 35]. For example, Du *et al.* have reported that pure MgH₂(110) surface has a hydrogen desorption energy barrier about 1.780 eV [29]. Wang *et al.* showed that the energy barrier of Ti doped MgH₂(110) surface was about 1.420 eV [31]. In addition, the energy barrier of Cu doped MgH₂(110) surface was about 1.480 eV as reported by Tang group [33]. Furthermore, Kumar *et al.* have investigated the energy barriers of metal (Ca, Sr, Ba, Al, Ga, In, Sc, Ti, V, Ni, Nb) doped MgH₂(110) surface, and found that In doped MgH₂(110) surface has a minimum energy barrier about 1.410 eV [35]. However, the adsorption properties of a single Pd atom on the MgH₂(110) surface have not been reported theoretically yet, and the microscope catalytic mechanism of the hydrogen desorption reactions of a single Pd atom adsorbed MgH₂(110) surface is still unclear.

In this work, we perform a theoretical research on the hydrogen desorption property of pure and a single Pd atom adsorbed MgH₂(110) surface. We compute the hydrogen desorption energies, energy barriers and temperatures of pure and a single Pd atom adsorbed MgH₂(110) surface. Furthermore, we discuss the microscopic process of the hydrogen desorption reactions through the reverse process of hydrogen spillover mechanism.

II. COMPUTATIONAL DETAILS

The first-principles density functional theory (DFT) calculations are performed with the Vienna *ab initio* simulation package (VASP) software package [36]. The generalized gradient approximation (GGA) of Perdew-Burke-Ernzerhof (PBE) [37] exchange correlation functional and the projector augmented wave (PAW) [38] method are used to describe the structural and electronic properties of the systems. The energy cutoff for the plane waves is set to be 400 eV. The convergence for the energy calculation is 0.0001 eV, and the structural optimization without any symmetry constraint is performed until the force is less than 0.01 eV/Å. For pure MgH₂(110) surface, the *x* and *y* directions are the period directions, and the vacuum with more than 18 Å is included in the *z* direction. The surface energy is calculated with 1×1 cell and 4×2×1 *k*-points. For the calculations of a single Pd atom adsorption on the MgH₂(110) surface and the hydrogen desorption energy barriers, 4×2 supercell and 1×1×1 *k*-point are used. We adopt the nudged elastic band (NEB) method to determine the energy barrier [39]. In addition, we also perform some test calculations for the hydrogen desorption energy barriers by using the van der Waals (vdW)

correction with the Grimme's method (DFT-D2) [40], and find that the vdW correction has only a little influence (within 0.1 eV) on the energy barriers in the calculations. Thus, our calculated results are based on the PBE calculations in this work.

III. RESULTS AND DISCUSSION

A. Pure MgH₂(110) surface

We first demonstrate the validity of our computational methods and structural models. The lattice parameters of the bulk MgH₂ crystal (space group P4₂/mmm (136)) are calculated to be $a=b=4.503$ Å and $c=3.005$ Å, which are in good accordance with previous experimental results ($a=b=4.517$ Å and $c=3.022$ Å) [4] and theoretical study ($a=b=4.500$ Å and $c=3.003$ Å) [41]. FIG. 1(a) shows that for the surface model, each H–Mg–H three atomic layer forms one trilayer in the *z* direction. MgH₂(110) surface with 4×2 supercell in the *x* and *y* directions and 3 trilayers (9 atomic layers) in the *z* direction is built. The bottom 2 atomic layers are fixed, and the top 7 atomic layers are relaxed in the calculations. The topmost surface atoms include the unsaturated twofold-coordinated bridge H atoms (indexed by BH, H_{2f}), saturated threefold-coordinated plane H atoms (indexed by PH, H_{3f}), unsaturated fivefold-coordinated Mg atoms (indexed by Mg_{5f}), and saturated sixfold-coordinated Mg atoms (indexed by Mg_{6f}). Our MgH₂(110) surface model totally has 48 Mg atoms and 96 H atoms (indexed by Mg₄₈H₉₆). It should be pointed out that the existence of the unsaturated bonds may affect the chemical properties of MgH₂(110) surface [29, 31, 33, 35].

We adopt 1×1 cell to calculate the surface energy of MgH₂(110) surface with 3, 4, 5 and 6 trilayers. The surface energy is 0.034 eV/Å² (between 0.0339 and 0.0341 eV/Å²), which is consistent with previous theoretical calculations (0.035 and 0.036 eV/Å²) [30, 33]. Therefore, the above surface model with 3 trilayers (see FIG. 1(a)) is enough to perform the surface calculations in this work.

B. A single Pd atom adsorption on the MgH₂(110) surface

We then study the structural and adsorption properties of a single Pd atom on the MgH₂(110) surface. Three type adsorption configurations are considered, including the surface, subsurface, and substitution adsorption models. FIG. 1 (b) and (c) show the surface, subsurface and substitution adsorption models of a single Pd atom on the MgH₂(110) surface with three trilayers. The surface adsorption models include the positions 1–6, and the subsurface adsorption models include the positions 7–9. The positions 7, 8, and 9 are

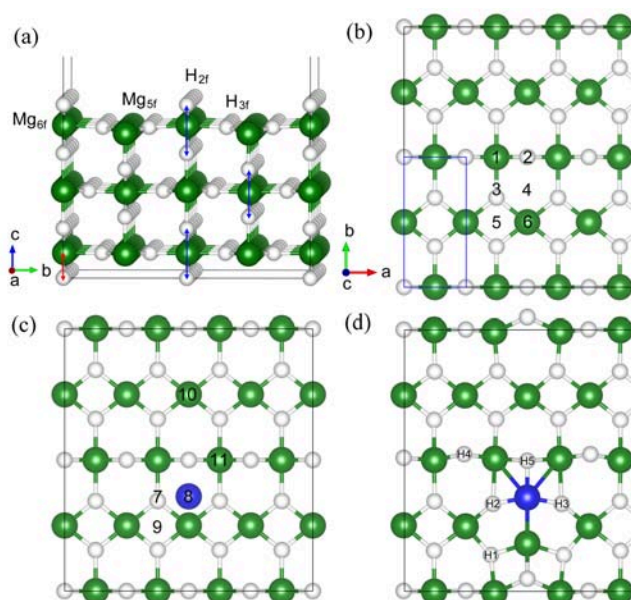


FIG. 1 (a) Pure $\text{MgH}_2(110)$ surface with 4×2 supercell and 3 trilayers (9 atomic layers) (side view). The trilayers are indicated by the blue arrows. The bottom two atomic layers (indicated by the red arrow) are fixed in the calculations. (b) The surface adsorption (positions 1–6) of a single Pd atom on the $\text{MgH}_2(110)$ surface, top view. The blue rectangle represents the 1×1 cell. (c) The subsurface adsorption (positions 7, 8, 9) and substitution adsorption (position 10, 11) of a single Pd atom on the $\text{MgH}_2(110)$ surface, top view. (d) Five hydrogen desorption paths of a single Pd atom adsorbed on the surface region of $\text{MgH}_2(110)$ surface, top view. The desorbed H atoms are indexed by H1, H2, H3, H4, and H5. For top view, only the topmost atoms are shown, and the other bottom atoms are omitted. Mg: green ball, H: white ball, Pd: blue ball.

below the positions 3, 4, and 5, respectively. In addition, for the substitution adsorption models, the positions 10 and 11 represent that the unsaturated Mg_{5f} and saturated Mg_{6f} atom are substituted by the single Pd atom.

The adsorption energy (E_{ad}) is defined as, for the surface and subsurface adsorption,

$$E_{\text{ad}} = E(\text{surface/Pd}) - E(\text{surface}) - E(\text{Pd}) \quad (1)$$

and for the subsurface and substitution adsorption,

$$E_{\text{ad}} = E(\text{surface/Pd}) - E(\text{surface}) - E(\text{Pd}) + E(\text{Mg}) \quad (2)$$

where $E(\text{surface/Pd})$, $E(\text{surface})$, $E(\text{Pd})$, and $E(\text{Mg})$ are the energy of the $\text{MgH}_2(110)$ surface with a single Pd atom, pure $\text{MgH}_2(110)$ surface, single Pd and Mg atoms from bulk Pd and Mg crystal, respectively [33, 35].

The adsorption energies of a single Pd atom on the $\text{MgH}_2(110)$ surface in different adsorption configurations are listed in Table I. The most stable position is

TABLE I The adsorption energy E_{ad} of a single Pd atom on the $\text{MgH}_2(110)$ surface, including the surface adsorption, subsurface adsorption, and substitution adsorption.

	Position	E_{ad}/eV
Surface	1	0.958
	2	1.814
	3	0.583
	4	0.190
	5	0.585
	6	0.731
Subsurface	7	-0.214
	8	-0.316
	9	1.426
Substitution	10	1.109
	11	0.987

the position 8 (subsurface), and the adsorption energy is -0.316 eV, indicating that a single Pd atom staying on the $\text{MgH}_2(110)$ subsurface has a lower energy by 0.316 eV compared with bulk Pd crystal.

The adsorption energy of the position 7 (subsurface) is -0.214 eV. However, the adsorption energy of the position 4 and 3 (surface) are 0.190 and 0.583 eV, respectively, which are both unstable compared with the bulk Pd crystal. We also find that the position 10 and 11 (substitution) have much higher energies, which indicates that the substitution adsorptions are more difficult than the surface and subsurface adsorptions. Therefore, our calculated results indicate that the single Pd atom prefers to stay on the subsurface region, and then on the surface region.

For the bulk MgH_2 crystal, the adsorption energies of a single Pd atom are calculated to be 0.360 eV. As shown in FIG. 2, $\text{MgH}_2(110)$ surface with four trilayers is used to calculate the adsorption energies of a single Pd atom staying from surface to subsurface, and then to inside (indexed by the positions 1–5). The position 2 is the most stable position, and its adsorption energy is -0.316 eV. When single Pd atom stays from subsurface to inside (positions 2–5), the total energy becomes higher. The adsorption energy of the position 5 is 0.363 eV, approaching to the value of a single Pd atom in the bulk MgH_2 crystal. In general, the calculated results of $\text{MgH}_2(110)$ surface with three and four trilayers are similar.

C. Hydrogen desorption reactions of pure $\text{MgH}_2(110)$ surface

For the hydrogen desorption reactions of pure $\text{MgH}_2(110)$ surface, four hydrogen desorption paths are chosen to perform the energy barrier calculations (see FIG. 1 (d)).

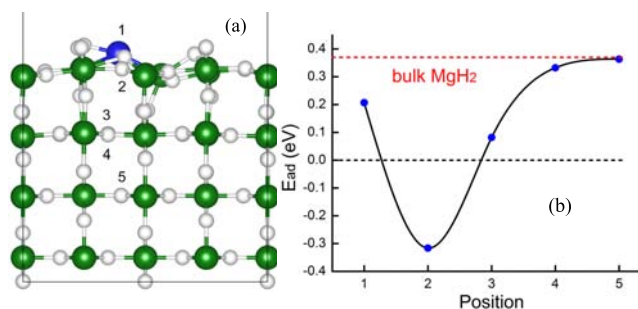


FIG. 2 (a) The adsorption positions of a single Pd atom on the $\text{MgH}_2(110)$ surface with 4 trilayers (side view). The single Pd atom from surface to inside is indexed by 1, 2, 3, 4, and 5, respectively. Mg: green ball, H: white ball, Pd: blue ball. (b) The adsorption energy E_{ad} of a single Pd atom on the $\text{MgH}_2(110)$ surface. Red dashed line represents the adsorption energy of a single Pd atom in the bulk MgH_2 crystal.

The hydrogen desorption energy (E_{d}) is defined as:

$$E_{\text{d}} = E(\text{FS}) - E(\text{IS}) \quad (3)$$

The energy barrier (E_{b}) is defined as:

$$E_{\text{b}} = E(\text{TS}) - E(\text{IS}) \quad (4)$$

where $E(\text{IS})$, $E(\text{TS})$, and $E(\text{FS})$ is the energy of the initio state (IS), transition state (TS), and final state (FS), respectively.

Table II lists the hydrogen desorption energies and energy barriers. The hydrogen desorption energies are 1.210, 2.187, 1.475, and 2.187 eV for the hydrogen desorption path 1, 2, 3, and 4, respectively. And the energy barrier is 2.172, 2.751, 1.802 (174 kJ/mol), and 2.863 eV for the path 1, 2, 3, and 4, respectively. Our calculated results are consistent with previous theoretical results (1.780, 1.830, 2.080, and 2.250 eV) [29, 31, 33, 35]. The experimental energy barriers of pure MgH_2 materials are observed to be around 161–188 kJ/mol [3, 5, 42, 43].

Furthermore, the path 3 is chosen as an example to simply explain the process of hydrogen desorption (FIG. 3). For the initio state, two H atoms coordinate with Mg atoms with the energy of 0 eV. Then, from the initio state to the transition state, two H atoms approach to each other gradually, and the energy increases to 1.802 eV for the transition state. And then, the energy becomes lower to 1.475 eV for the final state with a H_2 molecule desorbed to stay far away from the $\text{MgH}_2(110)$ surface.

Compared with the results of the path 1, the hydrogen desorption energy of the path 3 is higher by 0.265 eV, however, the energy barrier of the path 3 is lower by 0.370 eV. It should be pointed out that the chemical reaction rate has an inverse relationship with the energy barrier. Therefore, the probability of the occurrence for the path 3 is much higher than the path

TABLE II The hydrogen desorption energy E_{d} and energy barrier E_{b} of the path 1, 2, 3, and 4 for pure $\text{MgH}_2(110)$ surface. The desorbed H atoms are indexed by H1, H2, H3, H4, and H5.

Path	Atom	E_{d}/eV	E_{b}/eV
1	H2–H1	1.210	2.172
2	H2–H3	2.187	2.751
3	H2–H4	1.475	1.802
4	H4–H5	2.187	2.863

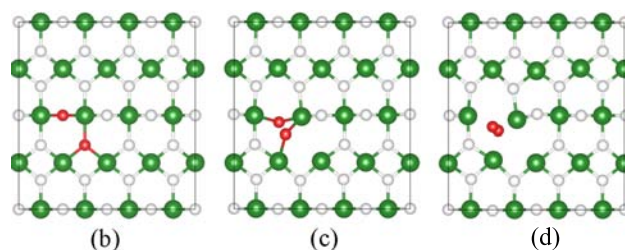
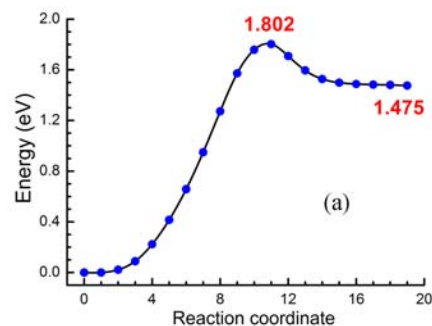


FIG. 3 (a) The energy profiles of the hydrogen desorption path 3 for pure $\text{MgH}_2(110)$ surface, (b) initio state, (c) transition state, and (d) final state (top view). Mg: green ball, H: white ball. Red balls stand for the desorbed two H atoms in the NEB calculation.

1 for hydrogen desorption reactions of pure $\text{MgH}_2(110)$ surface in the experiments.

D. Hydrogen desorption reactions of Pd adsorbed on the $\text{MgH}_2(110)$ subsurface

As mentioned above, the single Pd atom prefers to stay on the $\text{MgH}_2(110)$ subsurface. Five hydrogen desorption paths are chosen to perform the energy barrier calculations (FIG. 1 (d)). The hydrogen desorption energies and energy barriers are listed in Table III. The hydrogen desorption energy is 0.895, 1.181, 1.283, 2.002, and 1.005 eV for the hydrogen desorption path 1, 2, 3, 4, and 5, respectively. The energy barrier is 1.890, 1.743, 1.738, 2.506, and 1.649 eV for the path 1, 2, 3, 4, and 5, respectively. FIG. 4 shows the lowest energy barrier (1.649 eV) of the path 5.

Table III shows that for the same hydrogen desorption paths, the hydrogen desorption energies and en-

TABLE III The hydrogen desorption energy E_d and energy barrier E_b of the path 1, 2, 3, 4, and 5 for a single Pd atom adsorbed on the subsurface region of $\text{MgH}_2(110)$ surface. The desorbed H atoms are indexed by H1, H2, H3, H4, and H5.

Path	Atom	E_d/eV	E_b/eV
1	H2–H1	0.895	1.890
2	H2–H3	1.181	1.743
3	H2–H4	1.283	1.738
4	H4–H5	2.002	2.506
5	H3–H5	1.005	1.649

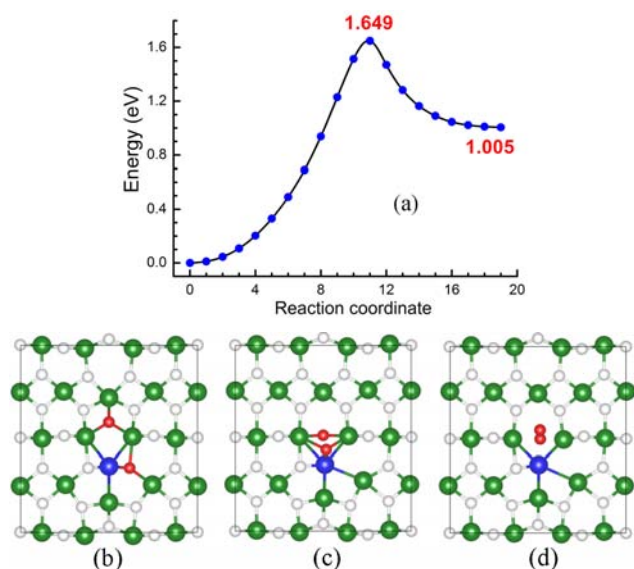


FIG. 4 (a) The energy profiles of the hydrogen desorption path 5 for a single Pd atom adsorbed on the subsurface region of $\text{MgH}_2(110)$ surface, (b) initio state, (c) transition state, and (d) final state (top view). Mg: green ball, H: white ball, Pd: blue ball. Red balls stand for the desorbed two H atoms in the NEB calculation.

energy barriers decreased on the existence of the single Pd atom, compared with Table II. When the single Pd atom stays on the $\text{MgH}_2(110)$ subsurface, it has a weak catalytic effect on the hydrogen desorption reactions, and the lowest energy barrier decreases by 0.153 eV, compared with the lowest energy barrier (1.802 eV) of pure $\text{MgH}_2(110)$ surface.

E. Hydrogen desorption reactions of Pd adsorbed on the $\text{MgH}_2(110)$ surface

Next, we consider the situation of the single Pd atom staying on the $\text{MgH}_2(110)$ surface. Five hydrogen desorption paths are chosen to perform the energy barrier calculations (see FIG. 1 (d)). The hydrogen desorption energies and energy barriers are listed in Table IV. The energy barrier of the path 2 and 3 is shown in FIG. 5

TABLE IV The hydrogen desorption energy E_d and energy barrier E_b of the path 1, 2, 3, 4, and 5 for a single Pd atom adsorbed on the surface region of $\text{MgH}_2(110)$ surface. The hydrogen desorption reactions include two steps. The hydrogen desorption energy of the first and second step is represented by E_{d1} and E_{d2} , respectively. The total hydrogen desorption energy is represented by E_{dt} . The desorbed H atoms are indexed by H1, H2, H3, H4, and H5.

Path	Atom	E_{d1}/eV	E_{d2}/eV	E_{dt}/eV	E_b/eV
1	H2–H1	0.809	0.175	0.984	1.607
2	H2–H3	0.974	0.282	1.257	1.198
3	H2–H4	0.986	0.011	0.997	1.154
4	H4–H5	1.191	0.008	1.199	1.407
5	H3–H5	1.146	0.205	1.351	1.247

and FIG. 6, respectively.

We find that the hydrogen desorption reactions include two steps. For the first step, the desorbed H_2 molecule stays near from the single Pd atom. For the second step, the H_2 molecule stays far away from the single Pd atom. The total hydrogen desorption energies are 0.984, 1.257, 0.997, 1.199, and 1.351 eV for the hydrogen desorption path 1, 2, 3, 4, and 5, respectively. The energy barriers are 1.607, 1.198, 1.154, 1.407, and 1.247 eV for the path 1, 2, 3, 4, and 5, respectively.

Compared with Tables II and III, Table IV shows that for the hydrogen desorption reactions, the minimum energy barrier is 1.154 eV (111 kJ/mol), 1.649 eV (159 kJ/mol), and 1.802 eV (174 kJ/mol) for the surface Pd atom, subsurface Pd atom, and pure $\text{MgH}_2(110)$ surface, respectively. Therefore, the surface Pd atom has a much stronger catalytic effect than the subsurface Pd atom.

We also consider the vdW correction with the DFT-D2 [40] for computing the energy barriers. For the DFT-D2 calculations, the energy barrier of the same hydrogen desorption path mentioned above is 1.115, 1.750, and 1.759 eV for the surface Pd atom, subsurface Pd atom adsorbed, and pure $\text{MgH}_2(110)$ surface, respectively. The differences of the energy barriers between normal PBE and PBE-vdW are within 0.1 eV, indicating that the vdW correction has only a little influence on the energy barriers in our calculations.

F. Discussion

For the hydrogenation and dehydrogenation process of Pd/Mg thin films, the general rules in experiments are that the energy barrier becomes higher as the Mg layer becomes thicker, however, the energy barrier becomes lower as the Pd layer becomes thicker. According to the different experimental conditions, the measured energy barrier values are within certain range, for example, 80 kJ/mol [8, 13], 61–77 kJ/mol [9], 60 kJ/mol [10],

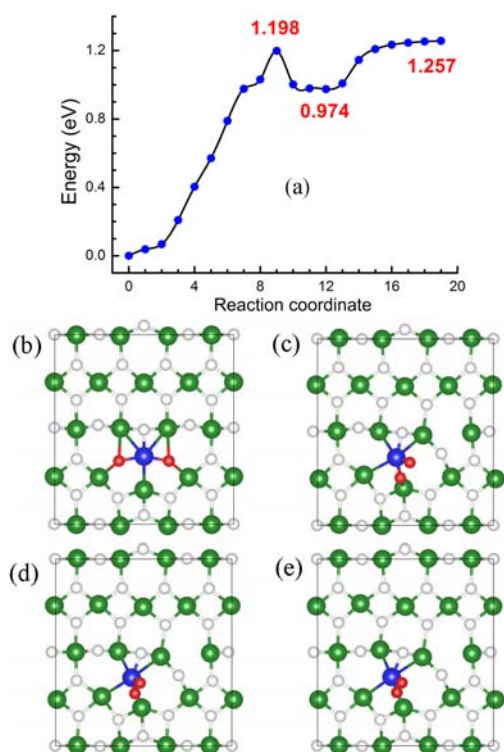


FIG. 5 (a) The energy profiles of the hydrogen desorption path 2 for a single Pd atom adsorbed on the surface region of MgH₂(110) surface, (b) initio state, (c) transition state, (d) final state (near), and (e) final state (far) (top view). Mg: green ball, H: white ball, Pd: blue ball. Red balls stand for the desorbed two H atoms in the NEB calculation.

48 kJ/mol [11], 118 kJ/mol [14], 122–135 kJ/mol [15], 37–49 kJ/mol [16]. It should be emphasized that our calculated lowest energy barrier is about 111 kJ/mol, which is included in the range of the experimental values. Furthermore, the Pd layers in the experiments have a large number of Pd atoms, however, our calculated results include only a single Pd atom. If more accurate energy barrier is required, more Pd atoms (Pd clusters, Pd layers) adsorption on the MgH₂(110) surface should be considered.

Experimentally, the reaction rate constant (k) is defined by the Arrhenius equation [42]:

$$k = k_0 \exp\left(-\frac{E_b}{RT}\right) \quad (5)$$

where k_0 is the pre-exponential factor, E_b is the energy barrier, R is the gas constant, and T is the absolute temperature. For the same chemical reaction, if the reaction temperature remains unchanged, as the energy barrier becomes lower, the reaction rate constant will become higher. In addition, if the reaction rate constant remains unchanged, as the energy barrier becomes lower, the reaction temperature will become lower. Experimentally, the standard hydrogen desorption tempera-

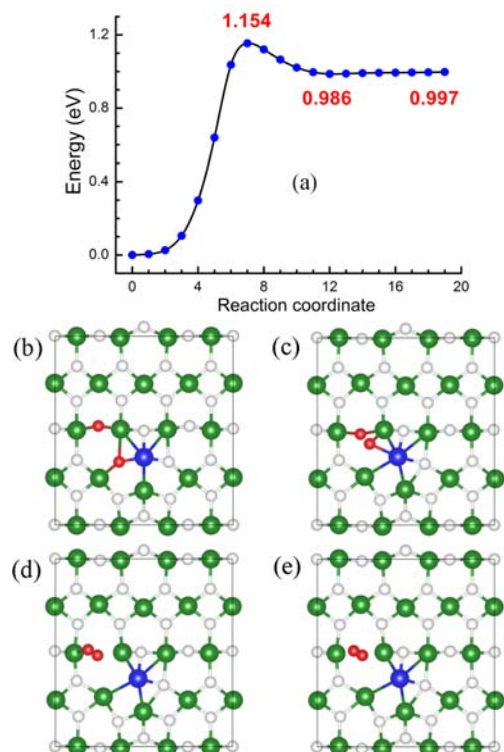


FIG. 6 (a) The energy profiles of the hydrogen desorption path 3 for a single Pd atom adsorbed on the surface region of MgH₂(110) surface, (b) initio state, (c) transition state, (d) final state (near), and (e) final state (far) (top view). Mg: green ball, H: white ball, Pd: blue ball. Red balls stand for the desorbed two H atoms in the NEB calculation.

ture (T_d) of pure MgH₂(110) is about 573 K (T_{d1}) at 1 bar H₂ pressure [44]. Considering the energy barrier 1.802 eV (E_{b1} =174 kJ/mol) for pure MgH₂(110) surface and 1.154 eV (E_{b2} =111 kJ/mol) for the single Pd atom adsorbed MgH₂(110) surface, through the equations:

$$k_1 = k_0 \exp\left(-\frac{E_{b1}}{RT_{d1}}\right) \quad (6)$$

$$k_2 = k_0 \exp\left(-\frac{E_{b2}}{RT_{d2}}\right) \quad (7)$$

if $k_1=k_2$, then

$$\frac{E_{b1}}{T_{d1}} = \frac{E_{b2}}{T_{d2}} \quad (8)$$

thus, the hydrogen desorption temperature (T_d) of the single Pd atom adsorbed MgH₂(110) surface is calculated to be 367 K (T_{d2}), indicating that the hydrogen desorption reactions could occur easily and quickly. The experimental values are between 360 and 475 K [6, 7, 12, 15]. Our calculated results are qualitatively consistent with the experimental values. Therefore, the existence of the single Pd atom significantly decreases

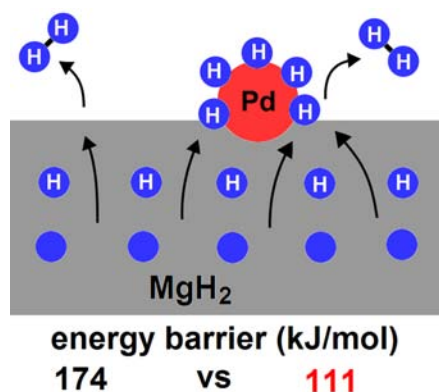


FIG. 7 The Pd single-atom catalysis to the hydrogen desorption reactions on the $\text{MgH}_2(110)$ surface.

the hydrogen desorption energy barrier and temperature of the $\text{MgH}_2(110)$ surface.

The intrinsic mechanism of such Pd single-atom catalysis to the hydrogen desorption reactions on the $\text{MgH}_2(110)$ surface can be understood through the reverse process of hydrogen spillover mechanism. Hydrogen spillover mechanism is typically defined as the dissociative chemisorption of hydrogen molecules (H_2) on transition metal catalysts (such as Ni, Ru, Pd, Pt), and the subsequent migration of the hydrogen atoms (H) from transition metal catalysts to the substrates (such as metal oxides including Al_2O_3 and TiO_2 ; various adsorbents including porous carbons, metal organic frameworks (MOF), covalent organic frameworks (COF), zeolitic imidazolate frameworks (ZIF), and other nanomaterials) [20, 24, 45–52].

In our work, we focus on the hydrogen desorption reactions, which are the reverse process of hydrogen adsorption reactions. FIG. 7 shows a simple description of the hydrogen desorption reactions of a single Pd atom adsorbed $\text{MgH}_2(110)$ surface through the reverse process of hydrogen spillover mechanism. In detail, single Pd atom adsorption on the surface attracts and adsorbs H atoms from inside MgH_2 , and makes them diffuse to the surface and activate around the Pd atom. Then two activated H atoms react to form one H_2 molecule under the Pd single-atom catalysis. Finally, these generated molecules can be desorbed from the surface by increasing ambient temperature in the experiments. It is obvious that the single Pd atom performs as a catalytic and active role for the hydrogen desorption reactions. Therefore, the single Pd atom significantly lowers the hydrogen desorption energy barrier from 174 kJ/mol for pure $\text{MgH}_2(110)$ surface to 111 kJ/mol for the single Pd atom adsorbed $\text{MgH}_2(110)$ surface, indicating that Pd is a promising catalyst to the hydrogen desorption reactions of the $\text{MgH}_2(110)$ surface.

IV. CONCLUSION

In summary, we perform a theoretical research on the hydrogen desorption reactions of pure and a single Pd atom adsorbed $\text{MgH}_2(110)$ surface. We find that a single Pd atom prefers to stay on the subsurface, and then on the surface. The lowest energy barrier of the hydrogen desorption reactions is 1.802 eV (174 kJ/mol) for pure $\text{MgH}_2(110)$ surface. While a single Pd atom exists on the subsurface, the lowest energy barrier is 1.649 eV (159 kJ/mol), indicating a weak catalytic activity. However, while a single Pd atom exists on the surface, the lowest energy barrier is only 1.154 eV (111 kJ/mol), indicating a strong catalytic effect. Furthermore, after the single Pd atom adsorption, the hydrogen desorption temperature decreases to 367 K (94 °C), which is much lower than pure $\text{MgH}_2(110)$ surface with 573 K (300 °C), indicating that the hydrogen desorption reactions will become much easier and quicker on the $\text{MgH}_2(110)$ surface. Our calculated energy barriers and hydrogen desorption temperature are qualitatively consistent with previous experimental results. At last, we discuss the microscopic process of the hydrogen desorption reactions through the reverse process of hydrogen spillover mechanism. Our computational results give out a reasonable explanation to prove that Pd has a very strong catalytic effect on the hydrogen desorption reactions of MgH_2 thin films, and offer a theoretical guidance for Pd/ MgH_2 thin films as good hydrogen storage materials in further experiments.

V. ACKNOWLEDGEMENTS

This work was supported by the National Key Basic Research Program (No.2011CB921404), National Natural Science Foundation of China (No.21421063, No.91021004, No.21233007, No.21803066), Strategic Priority Research Program of Chinese Academy of Sciences (No.XDC01000000) Research Start-Up Grants (No.KY2340000094) from University of Science and Technology of China, and the Chinese Academy of Sciences Pioneer Hundred Talents Program. We thank the USTCSCC, SC-CAS, Tianjin, and Shanghai Supercomputer Centers for the computational resources.

- [1] T. He, P. Pachfule, H. Wu, Q. Xu, and P. Chen, *Nat. Rev. Mater.* **1**, 16059 (2016).
- [2] E. S. Cho, A. M. Ruminski, Y. Liu, P. T. Shea, S. Kang, E. W. Zaia, J. Y. Park, Y. Chuang, J. M. Yuk, X. Zhou, T. W. Heo, J. Guo, B. C. Wood, and J. J. Urban, *Adv. Funct. Mater.* **27**, 1704316 (2017).
- [3] L. Zhang, L. Chen, X. Fan, X. Xiao, J. Zheng, and X. Huang, *J. Mater. Chem. A* **5**, 6178 (2017).
- [4] M. S. Tortoza, T. D. Humphries, D. A. Sheppard, M. Paskevicius, M. R. Rowles, M. V. Sofianos, K. F.

- AgueyZinsou, and C. E. Buckley, *Phys. Chem. Chem. Phys.* **20**, 2274 (2018).
- [5] Y. Zhang, X. Xiao, B. Luo, X. Huang, M. Liu, and L. Chen, *J. Phys. Chem. C* **122**, 2528 (2018).
- [6] H. Fujii, K. Higuchi, K. Yamamoto, H. Kajioka, S. Orimo, and K. Toiyama, *Mater. Trans.* **43**, 2721 (2002).
- [7] S. Singh, S. W. H. Eijt, M. W. Zandbergen, W. J. Leggerste, and V. L. Svetchnikov, *J. Alloys Compd.* **441**, 344 (2007).
- [8] J. Qu, Y. Wang, L. Xie, J. Zheng, Y. Liu, and X. Li, *J. Power Sources* **186**, 515 (2009).
- [9] G. Siviero, V. Bello, G. Mattei, P. Mazzoldi, G. Battaglin, N. Bazzanella, R. Checchetto, and A. Miotello, *Int. J. Hydrogen Energy* **34**, 4817 (2009).
- [10] J. Qu, B. Sun, Y. Liu, R. Yang, Y. Li, and X. Li, *Int. J. Hydrogen Energy* **35**, 8331 (2010).
- [11] J. Qu, B. Sun, J. Zheng, R. Yang, Y. Wang, and X. Li, *J. Power Sources* **195**, 1190 (2010).
- [12] Y. Liu and G. C. Wang, *Nanotechnology* **23**, 025401 (2012).
- [13] G. Xin, J. Yang, C. Wang, J. Zheng, and X. Li, *Dalton Trans.* **41**, 6783 (2012).
- [14] G. Xin, J. Yang, H. Fu, W. Li, J. Zheng, and X. Li, *RSC Adv.* **3**, 4167 (2013).
- [15] J. R. Ares, F. Leardini, P. DíazChao, I. J. Ferrer, J. F. Fernández, and C. Sánchez, *Int. J. Hydrogen Energy* **39**, 2587 (2014).
- [16] J. Qu, Y. Liu, G. Xin, J. Zheng, and X. Li, *Dalton Trans.* **43**, 5908 (2014).
- [17] G. Xin, Y. Wang, H. Fu, G. Li, J. Zheng, and X. Li, *Phys. Chem. Chem. Phys.* **16**, 3001 (2014).
- [18] G. Xin, H. Yuan, L. Jiang, S. Wang, X. Liu, and X. Li, *Phys. Chem. Chem. Phys.* **17**, 13606 (2015).
- [19] L. J. Bannenberg, H. Schreuders, L. van Eijck, J. R. Heringa, N. J. Steinke, R. Dalgliesh, B. Dam, F. M. Mulder, and A. A. van Well, *J. Phys. Chem. C* **120**, 10185 (2016).
- [20] S. Kumar, V. Singh, C. Cassidy, C. Pursell, C. Nivargi, B. Clemens, and M. Sowwan, *J. Catal.* **337**, 14 (2016).
- [21] K. Asano, R. J. Westerwaal, H. Schreuders, and B. Dam, *J. Phys. Chem. C* **121**, 12631 (2017).
- [22] V. D. Dobrovolsky, O. Y. Khyzhun, A. K. Sinelnichenko, O. G. Ershova, and Y. M. Solonin, *J. Electron Spectrosc. Relat. Phenom.* **215**, 28 (2017).
- [23] E. Hadjixenophontos, M. Roussel, T. Sato, A. Weigel, P. Stender, S. I. Orimo, and G. Schmitz, *Int. J. Hydrogen Energy* **42**, 22411 (2017).
- [24] S. Kumar, T. Pavloudis, V. Singh, H. Nguyen, S. Steinhauer, C. Pursell, B. Clemens, J. Kioseoglou, P. Grammatikopoulos, and M. Sowwan, *Adv. Energy Mater.* **8**, 1701326 (2018).
- [25] G. L. N. Reddy and S. Kumar, *Int. J. Hydrogen Energy* **43**, 2840 (2018).
- [26] K. Hassan and G. S. Chung, *Sens. Actuators B* **242**, 450 (2017).
- [27] X. Duan, S. Kamin, and N. Liu, *Nat. Commun.* **8**, 14606 (2017).
- [28] X. Duan and N. Liu, *ACS Nano* **12**, 8817 (2018).
- [29] A. J. Du, S. C. Smith, X. D. Yao, and G. Q. Lu, *Surf. Sci.* **600**, 1854 (2006).
- [30] J. H. Dai, Y. Song, and R. Yang, *J. Phys. Chem. C* **114**, 11328 (2010).
- [31] L. L. Wang and D. D. Johnson, *J. Phys. Chem. C* **116**, 7874 (2012).
- [32] E. Germán, V. Verdinelli, C. R. Luna, A. Juan, and D. Sholl, *J. Phys. Chem. C* **118**, 4231 (2014).
- [33] H. C. Wang, D. H. Wu, L. T. Wei, and B. Y. Tang, *J. Phys. Chem. C* **118**, 13607 (2014).
- [34] S. Kang, T. Ogitsu, S. A. Bonev, T. W. Heo, M. D. Allendorf, and B. C. Wood, *ECS Trans.* **77**, 81 (2017).
- [35] E. M. Kumar, A. Rajkamal, and R. Thapa, *Sci. Rep.* **7**, 15550 (2017).
- [36] G. Kresse and J. Hafner, *Phys. Rev. B* **49**, 14251 (1994).
- [37] J. P. Perdew, K. Burke, and M. Ernzerhof, *Phys. Rev. Lett.* **77**, 3865 (1996).
- [38] P. E. Blöchl, *Phys. Rev. B* **50**, 17953 (1994).
- [39] G. Henkelman and H. Jónsson, *J. Chem. Phys.* **113**, 9978 (2000).
- [40] S. Grimme, *J. Comp. Chem.* **27**, 1787 (2006).
- [41] Y. Lu, S. Dong, W. Zhou, Y. Liu, H. Zhao, and P. Wu, *J. Magn. Magn. Mater.* **441**, 799 (2017).
- [42] G. Chen, Y. Zhang, J. Chen, X. Guo, Y. Zhu, and L. Li, *Nanotechnology* **29**, 265705 (2018).
- [43] M. Jangir, A. Jain, S. Agarwal, T. Zhang, S. Kumar, S. Selvaraj, T. Ichikawa, and I. P. Jain, *Int. J. Energy Res.* **42**, 1139 (2018).
- [44] J. Zhang, S. Yan, and H. Qu, *Int. J. Hydrogen Energy* **43**, 1545 (2018).
- [45] H. Zhou, J. Zhang, D. Ji, A. Yuan, and X. Shen, *Micropor. Mesopor. Mater.* **229**, 68 (2016).
- [46] W. Karim, C. Sprefico, A. Kleibert, J. Gobrecht, J. VandeVondele, Y. Ekinci, and J. A. van Bokhoven, *Nature* **541**, 68 (2017).
- [47] S. K. Konda and A. Chen, *Mater. Today* **19**, 100 (2016).
- [48] C. J. Chung, C. Nivargi, and B. Clemens, *Phys. Chem. Chem. Phys.* **17**, 28977 (2015).
- [49] T. Liu, C. Chen, H. Wang, and Y. Wu, *J. Phys. Chem. C* **118**, 22419 (2014).
- [50] T. Liu, X. Ma, C. Chen, L. Xu, and X. Li, *J. Phys. Chem. C* **119**, 14029 (2015).
- [51] H. Nishihara, T. Simura, and T. Kyotani, *Chem. Commun.* **54**, 3327 (2018).
- [52] G. Zhan and H. C. Zeng, *Nat. Commun.* **9**, 3778 (2018).